Pergamon

Mechatronics Vol. 4, No. 7, pp. 653–671, 1994

0957-4158/94 $7.00+0.00

0957–4158 (94) 00033-6

AN IMPROVED FLEXIBLE PNEUMATIC JOINT FOR HORTICULTURAL ROBOTS

N. D. TILLETT,* N. VAUGHAN† and A. BOWYER†

*Silsoe Research Institute, Wrest Park, Silsoe, Bedford MK45 4HS, U.K. and
†University of Bath, Claverton Down, Bath BA2 7AY, U.K.

(*Received* 21 *April* 1994; *accepted* 31 *May* 1994)

Abstract—A previously reported novel rotary pneumatic actuator incorporating flexible inflatable elements has been improved. The attractions of this patented actuator (registered trade name "Flexator") for horticultural applications lie in its low cost and robust construction. Work fo improve its overall performance is described. This involved investigating and minimising sources of hysteresis, increasing torque-to-weight ratio and implementation of control techniques for dynamic positioning.

Two joints incorporating these principles have been constructed and linked to form a two-degree-of-freedom manipulator. Each link is 0.4 m long, has a 120° working stroke and moves in the horizontal plane. The manipulator, which weighs 8.5 kg, was tested with a 1.5 kg payload, which it positioned to within ± 2 mm in less than 1.5 s. It is concluded that the performance is adequate for the manipulator to demonstrate a simple horticultural fresh produce packaging application. This will form part of a programme of future work.

1. INTRODUCTION

An earlier paper [1] described work which established that it would be feasible to satisfy the requirements for a horticultural robot manipulator using a patented novel low-cost flexible rotary pneumatic actuator [2]. This paper describes subsequent work to find out in more detail those factors which affect actuator characteristics, and describes how they have been modified to better suit horticultural applications. Actuators based on a similar principle have also been investigated with a view to their use in rehabilitation robots [3].

In order to demonstrate the potential of such devices in commercial horticulture, a two-degree-of-freedom manipulator has been constructed. This configuration uses two joints, both working in a horizontal plane, and has been chosen for its simplicity and because of its suitability for commercially important tasks such as fresh produce packaging. Details of mechanical and controller design are given, leading to descriptions of manipulator construction and evaluation.

The background to this work is concerned with those tasks within horticulture which, for reasons of plant habit or susceptibility to damage, cannot yet be mechanised and rely on the dexterity and intelligence of manual labour. It is for these applications that robotics offers a way forward in the face of increasing labour costs and competition from imports. Examples of such applications include the harvesting of fruit, tomatoes and mushrooms, and the cutting of plant material for pruning or micropropagation as well as packaging and grading into presentation packs. Although

this variety does lead to some variation in ideal robot specifications, there are a number of general similarities, many of which are quite different from industrial requirements. In particular, a review of this subject [4] highlighted the need for flexibility between roles, and proposed that pneumatic actuators would best meet safety, hygiene and cost considerations. It was accepted that accuracy typically of the order of ±1 mm could be tolerated, which is lower than is normal in most industrial applications.

The actuator chosen to meet these needs was a rotary device based on flexible pneumatic elements. These elements are fabricated from layflat fire hose which is folded back on itself, the ends being clamped to form a seal. In the basic actuator (illustrated in Fig. 1) the hose is clamped with a length of webbing to a tube. The webbing and hose are then wrapped around the tube so that inflation of the hose causes the webbing to be pulled circumferentially. By connecting the free end of the webbing to an inner roller which rotates within the outer tube, rotary motion is produced. Two such arrangements working in opposite directions provide double-acting motion. In the earlier work a form of this actuator was constructed and tested with a PC based closed-loop controller using a modified PID (Proportional, Integral, Derivative) algorithm. The results were promising with steady-state accuracy of ±0.2° achieved.

2. MECHANICAL DESIGN

2.1. Experimental investigation of sources of hysteresis

2.1.1. Inflatable element. Earlier work revealed that the flexible actuator exhibited considerable hysteresis, which is known to make accurate dynamic control difficult. The sources of this hysteresis are thought to be sliding between components, and internal friction within woven materials, particularly where fibres can slide over one another (they stretch elastically). It has been shown that sliding between hose and outer tube can be minimised by restricting the angle that the fully collapsed hose subtends when wrapped around the outer tube to less than 120° [1]. Within this limitation the hose stays in direct contact with the outer roller. As the hose inflates and straightens, it rolls away from the cylinder without sliding motion. For larger wrap-round angles, kinks develop as the hose inflates causing sliding motion, energy loss, hysteresis and wear. Hysteresis as a percentage of output torque has also been shown to reduce with increasing operating pressure [1].

In order to further investigate the sources of hysteresis and to develop techniques for minimising them, a single-acting experimental rig was used. This rig was based on the configuration illustrated in Fig. 1, though only one hose was used. Angular displacement was monitored by a rotary potentiometer connected directly to the output shaft, and torque was measured by a load cell connected to the output arm and held perpendicular to it.

An important contributor to hysteresis is the woven synthetic hose material with its neoprene lining. Alternative materials with improved properties are not readily available, and so techniques for minimising undesirable effects must be sought. It was suspected that the kinks caused by folding the hose back on itself might contribute to friction during inflation. A single-thickness hose was therefore constructed by sealing

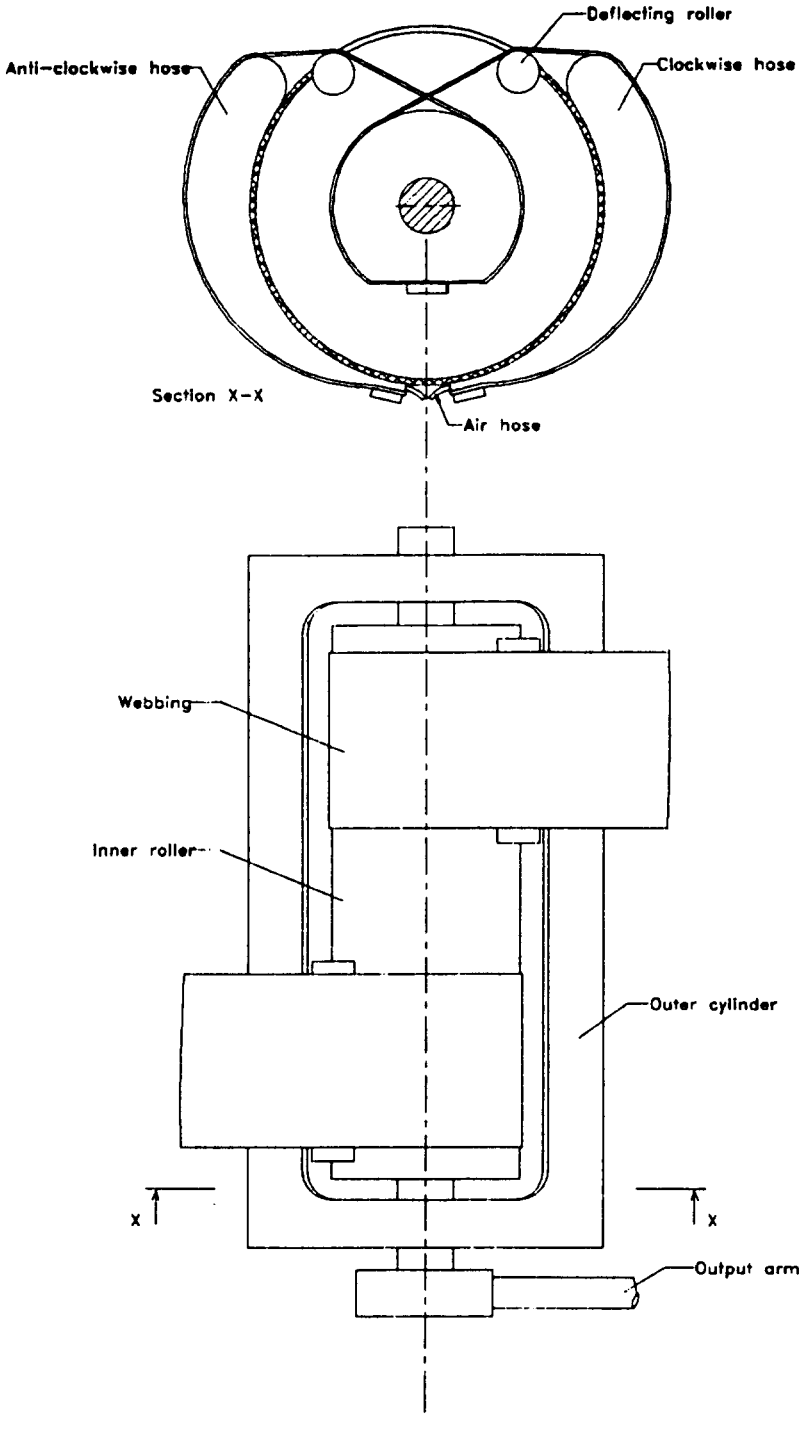

Fig. 1. Basic flexible actuator.

the two open ends with clamps which were pre-formed to the outer radius of the actuator. The hose was then clamped to the outer cylinder perpendicular to its normal orientation so that the cylinder and the hose axis were parallel. Webbing was then passed over the hose and connected to the inner roller in the normal way. Air entered the hose via a tube fixed by one of the end clamps. The results of the tests conducted in this configuration, which are illustrated in Fig. 2, showed no reduction in hysteresis compared to the standard configuration given in Fig. 3. Some fluctuation in measured torque in these and other figures can be explained by unsteadiness in holding the load cell by hand. These results suggest that folding the hose back on itself does not increase hysteresis and since this provides the mechanically most

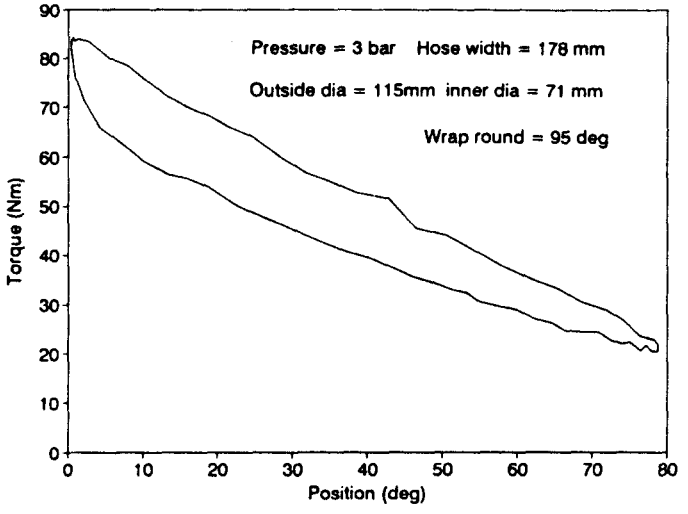

Fig. 2. Open-loop characteristic with single thickness of hose and polyester webbing.

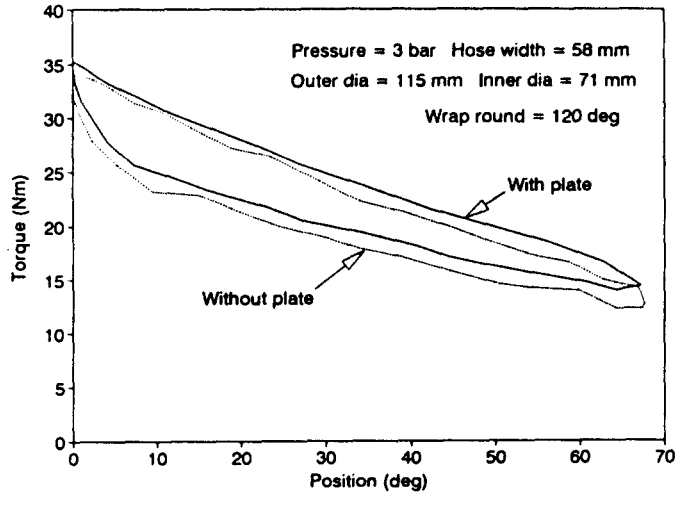

Fig. 3. Open-loop characteristic with polyester webbing with and without thin aluminium plate.

convenient means of clamping and sealing, it will continue to be used. Should other factors change, such as a requirement for long slender actuators, then this alternative geometry has been shown to be feasible.

Hysteresis in the hose only occurs when the material is distorted. One way of minimising hysteresis is to limit distortion to that which is required to provide actuator movement. As the hose inflates, in addition to providing circumferential movement, the outer surface of the hose swells up and becomes rounded. In order to limit this distortion, a 1.5 mm thick aluminium plate was placed between the hose and webbing. The plate, which was approximately pre-formed to the curvature of the hose around the tube, was held in place by friction. The function of the plate was therefore to keep the outer cross-section of the hose flat, but not to transmit tension or to modify circumferential profile. The results of comparative tests with and without the plate are given in Fig. 3. This shows a small reduction in hysteresis with the plate in place. It had been suggested that this reduction might be due, at least in part, to a reduction in friction between the two surfaces. To test this hypothesis the test was repeated replacing the aluminium sheet with two layers of polythene sheet. These, whilst not eliminating friction, would substantially reduce it and so indicate if this was a factor. The results did not show a noticeable reduction in hysteresis and so friction at the webbing interface is thought not to be a significant factor. This bears out earlier observations which indicated that for actuators of this geometry, there is no sliding movement between webbing and outer hose surface.

A development from using a thin plate between the hose and webbing is to constrain the hose with a rigid outer shell. It has been noted that the circular profile of the hose/webbing interface changes only slightly with actuator movement and so loads on the rigid outer shell can be expected to be relatively low. A potential advantage of the rigid outer shell which has not been quantified is that it will minimise the volume of the hose for a given output angle. This effect, though minor, may have a beneficial impact on dynamic performance. For the single-acting experimental rig, a rigid outer shell was constructed in aluminium with a radius equal to that of the fully collapsed hose. The shell which now transmitted tension had a simple webbing hinge attached to the hose clamp. The free end could then be attached to the inner roller by any flexible tension transmitting material. This did not need to be the full width of the hose.

2.1.2. Connecting strap. Looking now at alternatives to the webbing connecting the hose to the inner roller, high modulus materials were sought which had their fibres well aligned, so as to minimise internal friction as they came under tension. A plain woven polyaramid (Kevlar) 220 g/m^2 laminating cloth was folded, to provide a four-ply web with one weave parallel to the applied tension. The results which were taken with and without the thin aluminium plate are given in Fig. 4. This indicates that the Kevlar webbing is marginally superior to the conventional webbing and again shows the value of the aluminium plate.

Several types of wire and rope were tested in conjunction with the rigid outer shell. It was noted that multiple strands of thinner materials gave less hysteresis. This may be explained by distortion caused as the material was forced to pass under considerable tension over the 15 mm diameter deflecting rollers. Thinner materials will distort less and so create less hysteresis. With this in mind, thin strips of flexible steel sheet

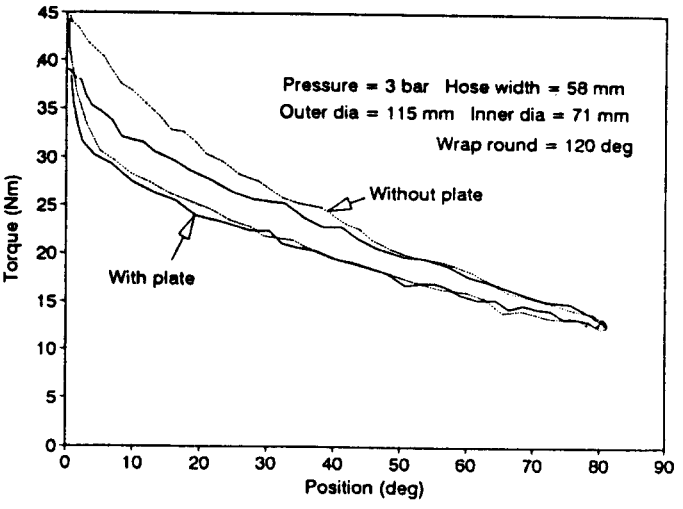

Fig. 4. Open-loop characteristic with Kevlar webbing, with and without thin aluminium plate.

were tried as an alternative to webbing or rope. High yield T301 sheet steel 0.1 mm thick by 46 mm wide was used in conjunction with the solid outer shell. The results (Fig. 5) give less hysteresis (approximately 8% at 3 bar) than any previous tests. This result contrasts with the hysteresis of approximately 21% revealed in tests with the polyester webbing alone, illustrated in Fig. 3. The high yield strength of the material, which was established to be 1.8 GN/m^2 in tensile tests, provides a high degree of design flexibility. The material did not show any signs of permanent bending where it passed over the deflecting rollers.

2.2. *Linearity*

The relationship between torque and displacement is determined by the ratio of inner roller to outer cylinder diameter. By replacing the circular section inner roller with a cam it is possible to modify further the torque–displacement characteristic. Mills [5] pointed out that since the output torque or force from actuators using flexible inflatable elements varies with position, it is normally necessary to vary pressure to compensate. Changing pressure also affects actuator stiffness and so stiffness in such actuators varies with position. Cam compensation allows the output torque to be modified so that it remains constant over the working stroke. Thus stiffness will not vary with position but could be controlled independently by altering supply pressure. The option to vary stiffness in this way has not been explored in this paper, and supply pressure remained constant for the experiments reported here. Cam compensation to provide constant output torque also simplifies the position-control algorithm. The desired cam profile can be derived using a graphical technique for the torque displacement relationship (Fig. 6). The basis of the technique is to relate the position of the outer shell to the tension in the material connecting shell to cam. For each shell-position/tensile-force a cam radius can be calculated. The position

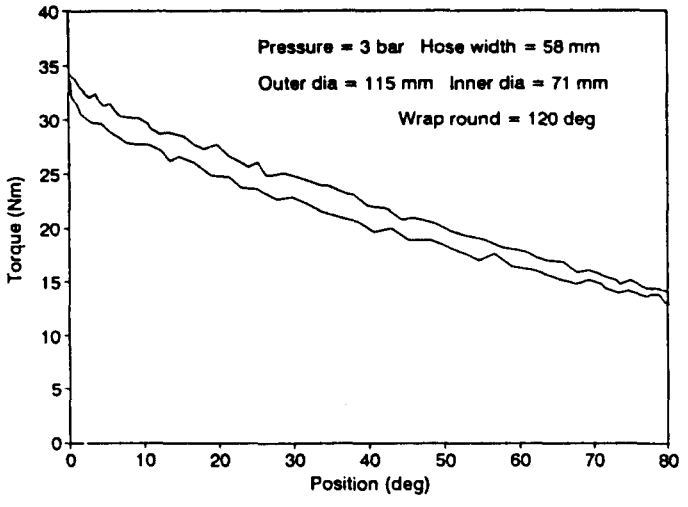

Fig. 5. Open-loop characteristic with solid outer shell and 0.1 mm thick steel connecting strap.

of the shell and the cam radius define the line along which the connecting material must act. The problem is then to relate this series of lines to cam output angles.

Where the relationship between force and outer shell displacement is simple, it is possible to integrate over the range of movement to derive an expression between cam angle and shell position as required. Where the expression is more complicated numerical integration techniques can be used.

For the geometry used in these actuators the output has been derived in an earlier paper to be [1]

$$T = \frac{PRr}{2\cos\left(\frac{\pi - \gamma}{2}\right)}\left(\pi R_h - R\left(\frac{\gamma - \alpha}{2}\right)\right)(1 - \cos\alpha), \tag{1}$$

where

T = output torque
P = pressure
R = outer cylinder radius
r = radius of round inner roller
R_h = cross-sectional radius of the fully inflated hose
γ = wrap-round angle fully deflated
α = hose angle to contact from clamp to point of break-away.

It has been determined experimentally that there is a constant ratio of approximately $1{:}1.3R/r$ between contact angle α and inner roller output angle. By substituting figures into these equations and calculating the work done for small increments of movement, it is possible to derive cam radii and displacements. By a process of crude numeric integration as illustrated in Table 1, the information required to plot the cam

Table 1. Theoretical prediction of flexible actuator characteristics and calculation of cam compensation parameters

System pressure	Hose width	Outer cylinder radius R	Inner roller radius r	Inflated hose radius R_h	Hose wrap-round angle g
400,000	0.16	0.0762	0.026	0.050955	2.094

Calculation of theoretical characteristics [Eqn (1)]							Output characteristics [from Eqn (1)]	
Angle (g)	Angle (a)	A	B	C	D	Z	Angle (b)	Torque (T)
2.094	2.094	0.866325	0.239945	0	1.499658	0.276969	0	109.7463
2.094	2.0312	0.866325	0.23109	0.002393	1.44431	0.262758	13.32	104.1153
2.094	1.9684	0.866325	0.221954	0.004785	1.38721	0.248539	26.64	98.48103
2.094	1.9056	0.866325	0.212573	0.007178	1.328584	0.234366	39.96	92.86506
2.094	1.8428	0.866325	0.202986	0.009571	1.268662	0.220291	53.28	87.28828
2.094	1.78	0.866325	0.193229	0.011963	1.207681	0.206367	66.6	81.77094
2.094	1.7172	0.866325	0.183341	0.014356	1.145881	0.192642	79.92	76.33252
2.094	1.6544	0.866325	0.173361	0.016749	1.083506	0.179163	93.24	70.99169
2.094	1.5916	0.866325	0.163328	0.019141	1.020802	0.165976	106.56	65.76616
2.094	1.5288	0.866325	0.153283	0.021534	1.958016	0.153121	119.88	60.67268
2.094	1.466	0.866325	0.143263	0.023927	1.895395	0.140639	133.2	55.72693

Intermediate values in the calculation of Eqn (1) (section 2.2)

$A = \cos((\pi - g)/2)$ $\quad B = \pi^* R_h(1 - \cos a)$ $\quad C = R(g - a)/(2^*\pi^* a)$

$D = \sin a - a^* \cos a$ $\quad Z = (B - C^* D)/A$ $\quad T = Z^* PRr/2$

Units: Pressure—newtons per square metre
Distance—metres
Force—newtons
Torque—newton metres
Angles—radians (except where stated otherwise)

as illustrated in Fig. 6 can be deduced. The same process could be applied to experimentally derived torque vs displacement data.

2.3. *Joint geometry and construction*

An important overall objective of this work is to produce a manipulator with adequate performance for horticultural applications, but at a lower cost than existing precision industrial robots. Simplicity and tolerance to misalignment in assembly are therefore important goals in mechanical design.

Dynamic performance is affected by component weight and becomes increasingly critical with distance from the main axis. Materials have for this reason been selected from aluminium alloys and plastics with steel only used in highly stressed components such as main shafts. The weight of the body of the large actuator is not relevant to the dynamic performance of the experimental actuator as it remains fixed. However, it too has been constructed using lightweight materials to provide flexibility for possible future applications in which it might be required to be mobile. Stress analysis has been elementary and restricted to manual calculations. Opportunities should therefore exist to reduce weights further through more sophisticated analysis.

Table 1—*continued*

$PRr/2$	a = angle of contact from clamp to point of break-away
396.24	b = uncompensated inner roller output angle = $(g - a)^*1.26^*/R/r$

	Work done	Numeric calculation of cam geometry					
		Move (m)	Force (F)	Crad	Cam angle	Cam deg	Output torque
	0	0	4221.011	0.019451	0	0	82.10202
	1424.318	0.006041	4004.433	0.020503	0.302419	17.33612	82.10202
	1349.291	0.012083	3787.732	0.021676	0.588885	33.75773	82.10202
	1274.365	0.018124	3571.733	0.022987	0.85942	49.26609	82.10202
	1199.821	0.024165	3357.242	0.024455	1.114105	63.86587	82.10202
	1125.934	0.030207	3145.036	0.026105	1.35308	77.56511	82.10202
	1052.969	0.036248	2935.866	0.027965	1.576543	90.37506	82.10202
	981.1792	0.04229	2730.449	0.030069	1.784743	102.3101	82.10202
	910.8072	0.048331	2529.468	0.032458	1.977982	113.3875	82.10202
	842.0827	0.054372	2333.565	0.035183	2.156611	123.6274	82.10202
	775.2214	0.060414	2143.343	0.038306	2.321027	133.0525	82.10202
Average torque (AT)	82.10202						

Intermediate values in the calculation of cam compensation parameters

Work done = torque (T)* change in angle (b)
Average torque (AT) = sum of work done/total stroke
move (m) = linear movement = $b^*r^*\pi/180$
Force (F) = webb tension = T/r
Crad = desired cam radius = AT/F
Cam angle = output angle = sum of: [change in m/average Crad]
Cam deg = cam angle in degrees
Output torque = F^*Crad

The size of the experimental manipulator for the type of application discussed in section 1 is not critical. A geometry using 0.4 m long arms each with a 120° working stroke has been chosen to cover a reasonable range of potential tasks. Mechanical stroke is 140° to prevent limits being reached during overshoots. The nominal design payload was 1 kg. Actuator sizing was based on the performance of the first experimental device [1], and predicted component weights. Expected improvements in dynamic characteristics, together with material size availability also influenced the choice, which was for 85 and 25 Nm maximum torques at 4 bar for the inner and outer arms respectively. In the larger joint 160 mm wide hose is wrapped 120° round a 152 mm diameter outer cylinder. The smaller joint uses 110 mm hose, wrapped 120° round a 102 mm cylinder.

In this and most other applications it is desirable to make the manipulator and therefore its joints as compact as possible. To this end, it was decided to mount the opposing hoses back to back as illustrated in Fig. 7. Solid outer shells have been used with two connecting steel strips interleaved from each side. Careful selection of steel strip length ensures that the hose itself starts to be compressed before the output arm reaches its mechanical limit, thus providing a safety bump stop.

It proved very difficult to accommodate deflecting rollers of adequate diameter, and so the main output shaft axis was offset. This allowed the connecting steel strip to go directly from outer shell to cam, reducing one source of hysteresis and component wear. Having made this change, it would be possible to consider mounting the hose

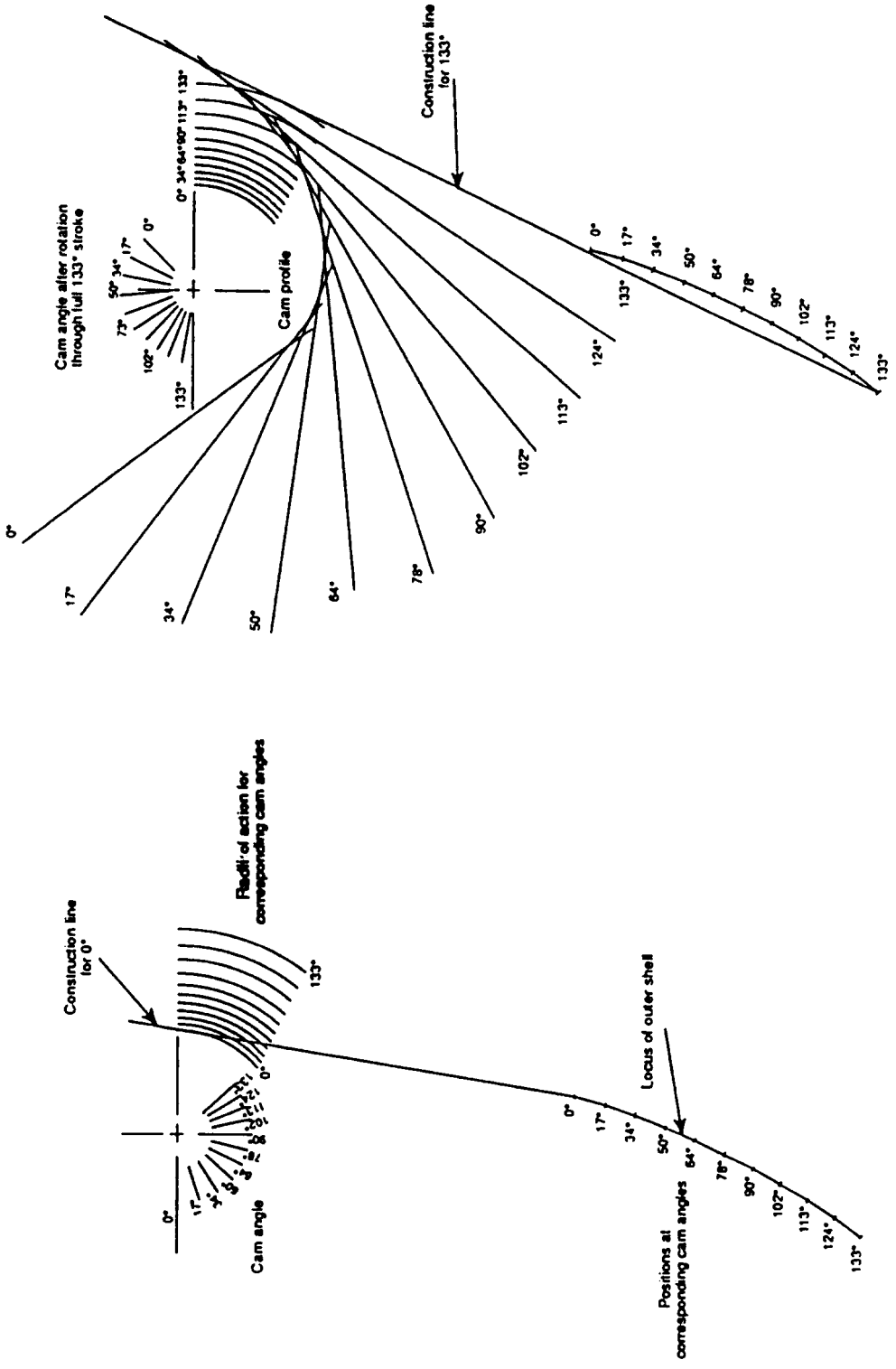

Fig. 6. Cam plotting procedure.

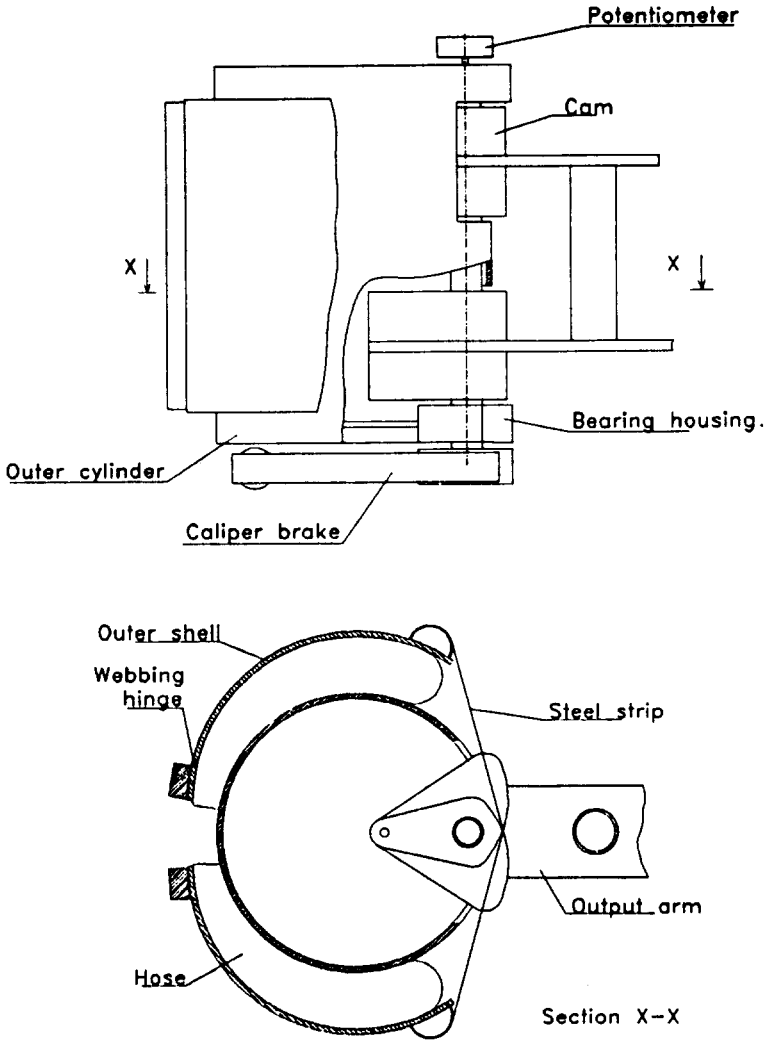

Fig. 7. Improved flexible actuator.

on flat or curved plates either side of the output shaft instead of round a tube. It has been calculated that the torque–displacement characteristics would be acceptable. However, the outer cylinder arrangement has been retained as it is structurally superior.

The provision of an offset output shaft allows the output arm to be connected directly to the cams. This simplifies the design and reduces overall length. Torque is no longer transmitted through the shaft allowing significant weight reductions to be made. The assembly, which effectively combines the structure of the actuator with the mechanical requirements of the entire joint, is illustrated in Fig. 7.

It is known that the addition of coulomb friction to a system has a stabilising influence, though at the expense of other dynamic characteristics. Provision was therefore made for a brake on the output shaft which could be used in experiments,

but removed easily if not required. A calliper type brake was designed which fitted on the underside of the joint and acted on an aluminium disk attached to an extension of the main output shaft (Fig. 7). The callipers were held against the disk by a coil spring, though a small pneumatic actuator could be used and would allow easy adjustment of braking torque, even as part of a dynamic control algorithm. The nylon brake material was chosen for its ability to provide coulomb friction with little stiction.

The two actuators are linked by a simple space frame. The complete assembly is shown in Fig. 8.

3. CONTROL

Joint position was controlled by apportioning air between opposing hoses using a solenoid-operated proportional-flow-control spool valve. Within the valve driver, current to the solenoid is controlled by the summation of three voltage levels. One is a simple zero adjustment and the second is the controlling signal from a D/A channel of a 386 PC. The third is a PC generated pseudo-sine wave dither signal designed to cause the valve spool to oscillate, so minimising the effect of spool friction.

Two feedback signals are generated, one from a potentiometer mounted on the

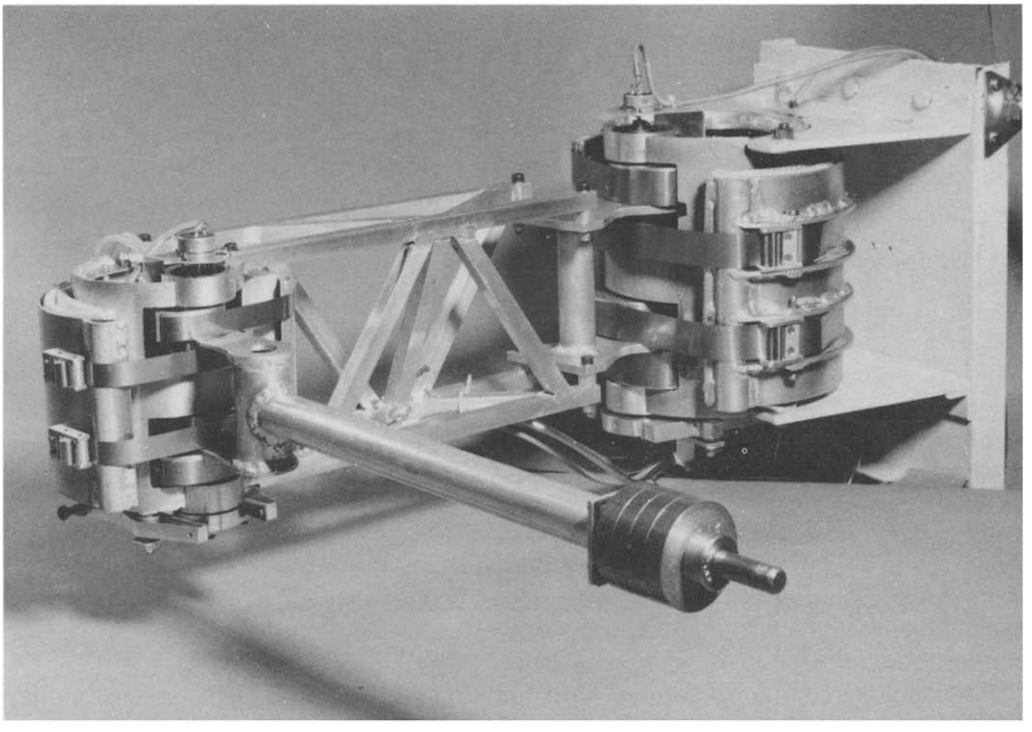

Fig. 8. Two-axis manipulator.

output shaft, giving angular position, and another from a pressure transducer measuring differentially between hoses. These analogue signals are converted to 12-bit resolution digital signals. Differential pressure feedback, which is analogous to acceleration, is used as a damping term. This is used in preference to the first or second differential of the position signal which would result in a noisy output. In this case, it is thought more economical to employ two low-cost sensors than a single high-cost device such as a high resolution optical encoder which may be less robust. A schematic of the system is presented in Fig. 9.

Like the control system described above the controlling algorithm is based on the one reported earlier [1]. The controlling equation can be represented as follows:

$$V[n] = k_e[n][\,](x - d) + k_p[n][\,]\Delta_p + N[n] + F[n](x - d) + FL[n](x - d), \quad (2)$$

where

V = output voltage to valve
k_e = proportional to error gain
k_p = proportional to differential pressure gain
x = actual position
d = demand position
n = array index indicating axis number
[ ] = indicates an array whose values vary with error and output velocity
N = null value
$F(x - d)$ = short-term integration of error function
$FL(x - d)$ = long-term integration of error function
Δ_p = differential pressure.

One modification has been the addition of a long-term integral. This slow acting term corrects for long-term variations in neutral values within the system as a whole. These variations might be electrical or mechanical in nature, due perhaps to temperature changes or wear, for example. The rate of build up of this long-term integral is governed by a number of rules. These include the following.

(1) The presence of an air supply, which is deduced by detecting pressure ripple caused by valve spool oscillation.
(2) The attainment of equilibrium indicated by low velocity.
(3) The absence of an offset load indicated by a low absolute differential pressure.

The principal modification between the algorithm described here and the one reported earlier relates to the need for multiple axes. This has been achieved by converting variables to arrays and running the controlling algorithm more than once per cycle. Each cycle is triggered by a hardware interrupt, set at 5 ms intervals. The code, which is written in C, has not been optimised for speed, but would be capable of running at at least twice this rate when operating two axes.

The manipulator joints described in this paper are capable of responding to the 50 Hz spool dither signal when unbraked. To avoid aliasing problems, it is necessary to sample feedback signals over the full 20 ms wavelength. This produces a time delay in the feedback loop of the same order as the speed of response of the system and is likely to have an adverse effect on control. The simplest solution would be to eliminate the dither signal or raise its frequency significantly. Unfortunately, the valve

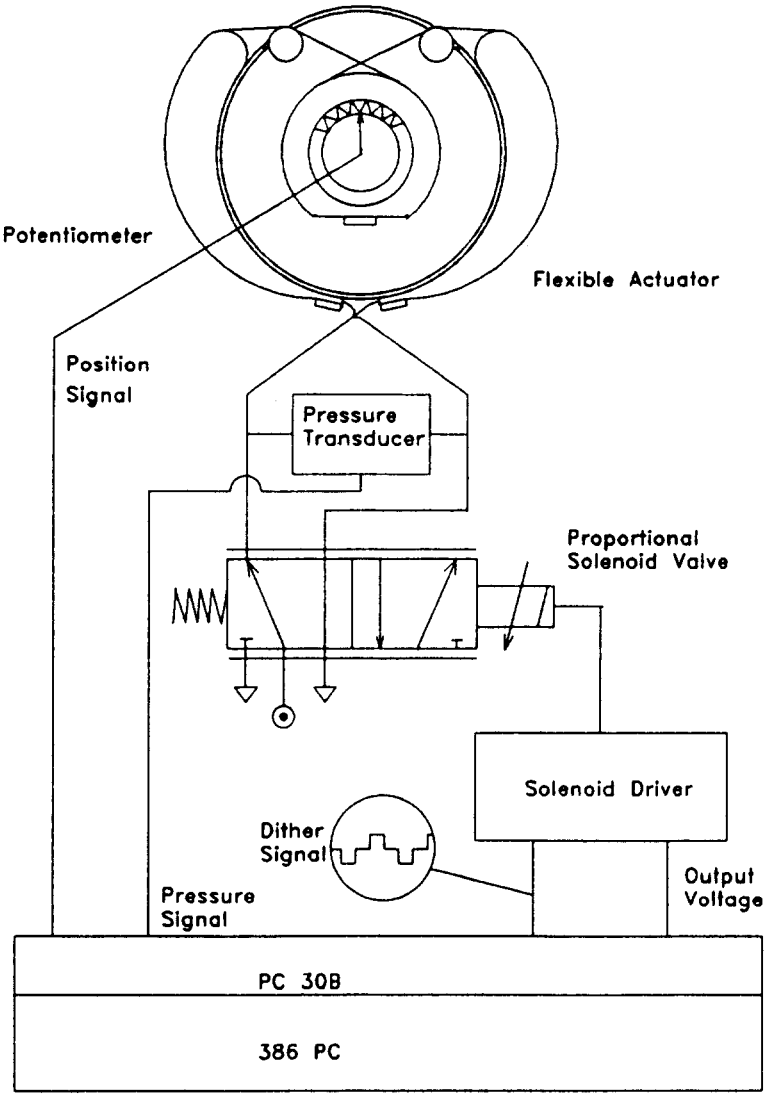

Fig. 9. Schematic showing a single axis only.

suffers from friction induced hysteresis without dither and starts to assume the characteristics of an on/off valve at higher dither frequencies [6].

The addition of coulomb friction braking eliminates mechanical joint movement due to the 50 Hz dither component, but it remains on the differential pressure signal, thus providing a partial solution only. Alternative valves are being sought, though the performance reported here relates to the system as described above.

Tuning is conducted in an empirical way, taking one joint at a time and considering each phase of position control in turn. Each position move has been divided into three phases. The first phase relates to a situation with high error and/or velocity. In

this phase, proportional-to-error gain is relatively low and the differential pressure damping term high, to ensure absolute stability coupled with an adequate rate of response. In the second phase, where error and velocity are moderately low, proportional gain is increased and damping reduced. The third phase equates to a situation where the joint has almost settled close to the desired position. In this case, proportional gain is increased markedly to reduce steady state error. Differential pressure damping is reduced (possibly to zero if mechanical damping is adequate), which reduces any steady state errors caused by zero errors in differential pressure. Also in this third phase, a short term integrator is introduced, further reducing steady state error.

4. EXPERIMENTAL EVALUATION

4.1. One-degree-of-freedom joint

The results of an evaluation of the performance of a single joint are presented in this subsection. The smaller of the two joints has been chosen for this purpose and is compared to the experimental actuator previously reported [1]. The most obvious differences lie in the reduced bulk and weight of the new joints, the smaller of which measures 18 cm high, weighs 2 kg including the brake assembly and has a maximum output torque of 27 Nm at 4 bar. The larger joint is 25 cm high, weighs 5.5 kg, with a 84 Nm torque at the same pressure.

The open-loop characteristics of a single hose from the smaller joint are given in Fig. 10 and can be compared with the equivalent characteristics of the previously reported actuator in Fig. 11. The success of the design features mentioned earlier is clearly visible with hysteresis down from 25 to 7%. Closed loop characteristics were however less favourable, as the new joint, whilst stable, takes several seconds to settle down and is prone to small amplitude oscillations.

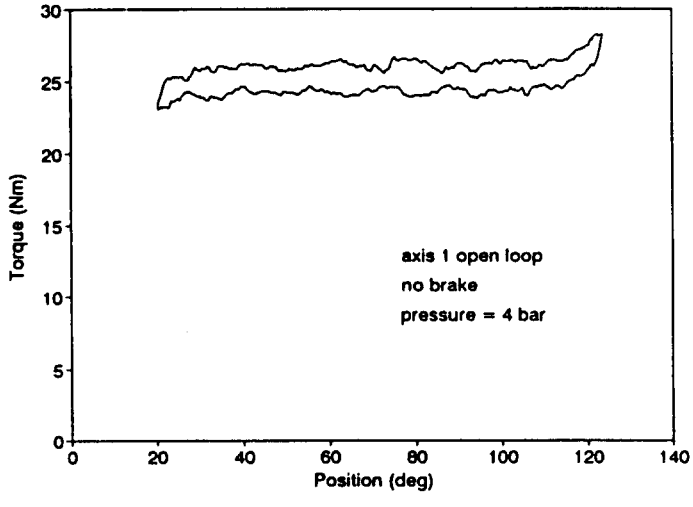

Fig. 10. Open-loop characteristic of axis one without braking.

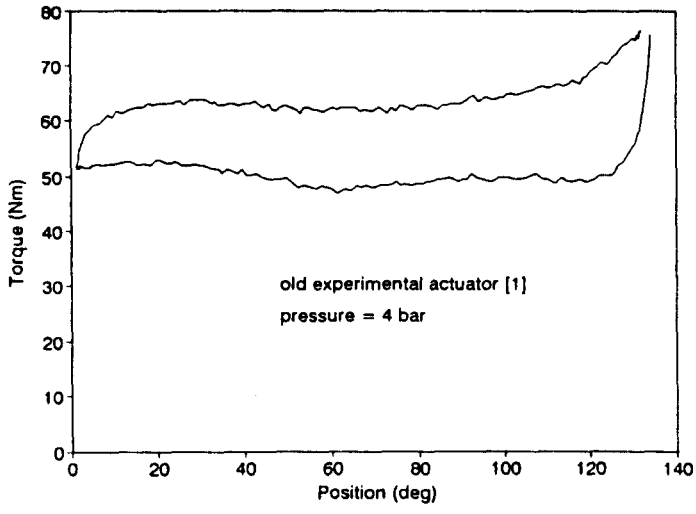

Fig. 11. Open-loop characteristic of old experimental actuator [1].

The reduced stability has been attributed to the lower hysteresis in the new joint, as all other factors were set up to be equivalent. The control algorithm was essentially the same and the inertial payload/output torque ratio was the same at 10^{-2} kgm^2/Nm. To test this hypothesis, the calliper brake on the new joint was adjusted to bring the hysteresis back up to 25% through the addition of coulomb friction. The resulting open-loop characteristic is given in Fig. 12 and clearly shows the difference between coulomb friction induced hysteresis and that present in the original actuator. Coulomb friction imposes a force which is constant in magnitude but whose polarity is dependent on the direction of motion no matter how fast or slow. Idealised coulomb

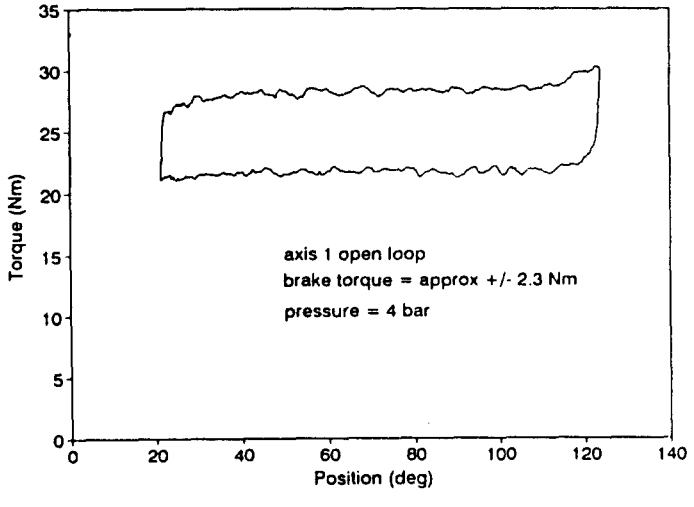

Fig. 12. Open-loop characteristic of axis one with braking.

friction would give a rectangular hysteresis characteristic with vertical sides. Thus in a system with coulomb friction, small amplitude oscillations are opposed by the full hysteresis force. The characteristic of the original actuator in Fig. 11 shows that the magnitude of the hysteresis force opposing is dependent on the size of the movement. Thus small amplitude oscillations are opposed by forces lower than full hysteresis, giving a reduced damping effect.

As anticipated, the coulomb friction improved stability, but to a level greater than seen in the original actuator. Figure 13 demonstrates a stable response in this configuration with a 0.32 kgm^2 payload which, relative to actuator size, is approximately double that which was the stability limit for the original actuator. It is concluded that coulomb friction improves stability and that its benefits can outweigh the hysteresis caused. Where a substantial part of the hysteresis is not due to coulomb friction the benefits are significantly less. On this basis, it remains beneficial to design for minimum hysteresis and to add coulomb friction in a controlled way at the tuning stage. Coulomb friction between piston and cylinder in conventional pneumatic linear actuators is also known to improve stability in position control applications.

4.2. Two-degree-of-freedom manipulator

The two-degree-of-freedom manipulator illustrated in Fig. 8 weighs approximately 8.5 kg, excluding valves and payload. Although its response is to some extent dependent on geometric configuration, Fig. 14 gives a typical result for step changes in demand position for each axis in turn. This shows that although movement of the smaller joint has little effect on the larger joint, the reverse is not true. The steady state accuracy is not affected, however, and is reached within about 1.5 s with 1.5 kg payload. The manipulator is repeatable to ±0.1° on each joint, which corresponds to about ±1–2 mm depending on geometry. The brakes on both joints have been set up to provide coulomb friction corresponding to approximately ±8% of maximum output

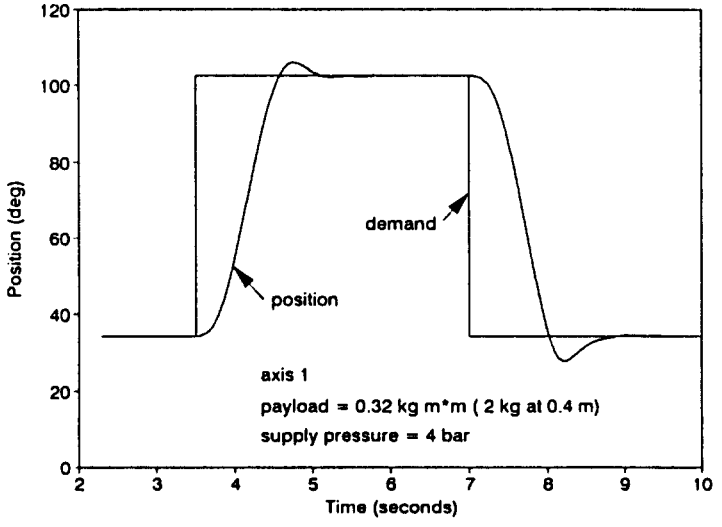

Fig. 13. Closed-loop response of axis one with 2 kg payload.

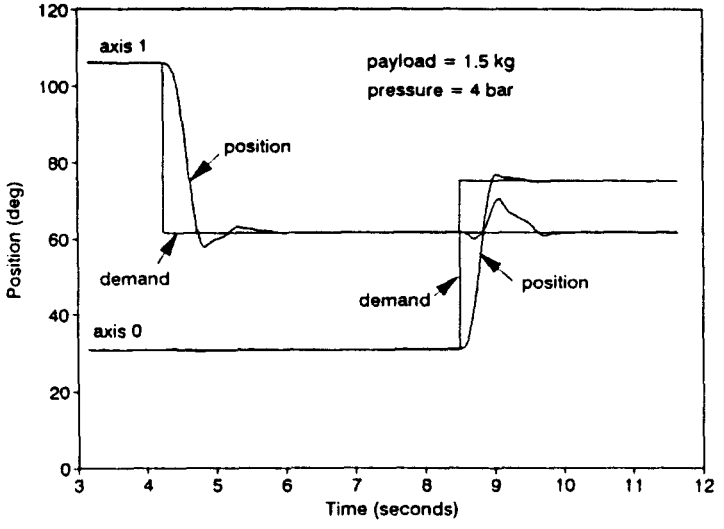

Fig. 14. Closed-loop response of two-axis manipulator with 1.5 kg payload.

torque. Overall hysteresis is approximately 25% in both cases. This includes the element due to internal distortion within the hose material, as well as the deliberately applied coulomb friction.

5. CONCLUSIONS

An experimental investigation with an experimental flexible actuator has shown that the flexible hose material itself and the webbing connecting the hose to the output shaft are both major sources of hysteresis. A new design with improved geometry and better choice of materials has reduced hysteresis from approximately 25 to 7%. Weight and bulk have also been reduced so that output torque/joint mass is now 3.5 Nm/kg per bar supply pressure.

Small amplitude oscillations in the new joint proved difficult to dampen without the addition of coulomb friction. Coulomb friction at ±8% of maximum output torque provided adequate stability and made satisfactory dynamic performance possible. The hysteresis induced by coulomb friction, whilst similar in magnitude to that eliminated by the design changes, is different in nature, particularly with respect to dynamic damping. As a result of these modifications, a joint can carry an inertial load of approximately 10^{-2} kgm^2 per Nm of output torque.

Two such joints have been combined to form a two-degree-of-freedom manipulator with two 0.4 m long links. The total weight is 8.5 kg excluding pneumatic valves, control equipment and the end effector. Satisfactory performance has been demonstrated with a 1.5 kg payload positioned to within ±2 mm inside 1.5 s.

The experimental manipulator will now be demonstrated conducting a simple horticultural fresh produce packaging task involving the use of computer vision for target identification. Whilst the existing dynamic performance is adequate for this

purpose the same is not so for applications that require tracking of moving objects, or working with varying offset loads. These are both requirements for a general purpose horticultural manipulator and so further work is required. In particular, it is necessary to investigate the role of coulomb friction in dynamic performance and the choice of valve to eliminate or minimise the detrimental effects of dither signals.

Acknowledgements—This project is funded by the Ministry of Agriculture, Fisheries and Food. The flexible actuator, registered trade mark "Flexator", has been used with the permission of Airmuscle Ltd.

REFERENCES

1. Tillett N. D., Flexible pneumatic actuators for horticultural robots—a feasibility study. *Mechatronics* **3**, 315–328 (1993).
2. Hennequin J. R. and Fluck P., Motorised joint. International Patent classification PCT/GB87/00473, Filing date 21 October (1987).
3. Prior S. D., Warner P. R., White A. S., Parsons J. T. and Gill R., Actuators for rehabilitation robots. *Mechatronics* **3**, 285–294 (1993).
4. Tillett N. D., Robotic manipulators in horticulture; a review. *J. Agric. Engng Res.* **55**, 89–105 (1993).
5. Mills J. K., Hybrid actuator for robust manipulators: design, control and performance. *Mechatronics* **3**, 19–38 (1993).
6. M/2999 Proportional solenoid operated flow control valve. Data sheet. Norgren Martonair Ltd (1990).